Arabian Journal of Chemistry (2021) **14**, 103064

King Saud University

Arabian Journal of Chemistry

www.ksu.edu.sa
www.sciencedirect.com

ORIGINAL ARTICLE

Adsorption of chromium (VI) and iron (III) ions onto acid-modified kaolinite: Isotherm, kinetics and thermodynamics studies

P. E. Dim [a,*], L. S. Mustapha [a], M. Termtanun [b], J. O. Okafor [a]

[a] *Chemical Engineering Department, Federal University of Technology, Minna, Nigeria*
[b] *Chemical Engineering Department, Silpakorn University, Nakhon Pathorn 73000, Thailand*

Received 17 October 2020; accepted 4 February 2021
Available online 18 February 2021

KEYWORDS

Chromium (VI);
Iron (III);
Kaolinite;
Isotherm;
Adsorption;
Thermodynamics

Abstract The pollution of aquatic bodies by heavy metals effluent from many industrial activities is a significant environmental challenge affecting the ecosystem. Batch process was conducted to remove Cr (VI), and Fe (III) with hydrochloric acid modified clay (HMC) and acetic acid modified clay (AMC). The adsorbents morphology, chemical properties were measured by scanning electron microscope (SEM), X-ray fluorescence spectrometry (XRF), cation exchange capacity (CEC), X-ray diffraction (XRD) and Brunauer-Emmett-Teller (BET). The effects of time, adsorbent dose, temperature and pH of effluent on adsorption were studied. The acid activation increased the BET surface area from 84.223 m^2/g raw clay (RC) to 389.37 m^2/g (HMC) and 319.955 m^2/g (AMC), total pore volume increased to 0.2168 and 0.2285 cm^3/g, respectively. The CEC increased from 8.4 cmol/g to 22.30 cmol/g (HMC) and 20.73 cmol/g (AMC). The results of XRF, SEM and XRD studies show disintegration and a porous structure of the treated clay, and also changes in the intensity of the bands. The HMC had a maximum removal of Cr (VI), and Fe (III) of 79% and 90% at pH 7.0 and AMC recorded 60% and 57% at pH 6.0, respectively. The adsorption process equilibrium was attained at 50 and 90 min for HMC and AMC, respectively. Langmuir isotherms had the best fit. HMC and AMC adsorption capacity are, Cr (VI):18.15 mg/g and Fe (III):39.80 mg/g; Cr (VI): 10.42 mg/g and Fe (III):19.34 mg/g. The interaction of Cr (VI) and Fe (III) ions onto HMC/AMC was spontaneously endothermic. It agreed with the second-order equation. The maximum desorption efficiency recorded on HMC is 92.45 and 85.67% for Cr (VI) and Fe (III) and for

* Corresponding author.
E-mail address: pevdim@yahoo.com (P.E. Dim).
Peer review under responsibility of King Saud University.

Production and hosting by Elsevier

https://doi.org/10.1016/j.arabjc.2021.103064

AMC is 76.58 and 65.32% for Cr (VI) and Fe (III). The process is economically important because it provides an avenue for safe disposal or reuse of adsorbent. This attempt has shown the potential of modified clay as a suitable eco-friendly sorbent for removing heavy metals.

1. Introduction

The pollution of aquatic bodies by heavy metal discharged from various industrial activities is a global environmental challenge. Most industries in third world nations make little or no provision to treat their effluent before discharging it. Their presence in the water bodies in above acceptable limit is a serious hazard on human and ecosystem since they are non-biodegradable and can persist in different environmental conditions. Therefore, it is essential to protect the environment and the public from these pollutants by removing them from the aquatic ecosystem. The heavy metals in focus are chromium (VI) and Fe (III) ions. Chromium finds application in chrome plating, pigment, textile, wood preservation, and as antifouling agent in cooling towers (Li et al., 2016; Shen et al., 2012). The versatility of chromium has increased its concentration, especially in water bodies. Chromium (VI) ion presence in water above permissible level is poisonous and can cause diseases like cancer, kidney and liver failure (Rai et al., 2016, Ciopec et al., 2012). Therefore, it necessary to treat any wastewater containing chromium (VI) to the permissible level. According to the world health organization (WHO), the limit for drinkable water is 0.05 mg/L, and wastewater from industries is 0.5 mg/L (WHO, 2017). The primary source of ferric metallic ions is the ore mining activities, which comprises various minerals and heavy metals. The mining waste at oxidized state is corrosive and leads to acid mine drainage. It contains arsenic, copper, lead, cadmium, iron, sulfates. Ferric ions are highly present in acid mine drainage waters in a concentration of several 100 mg/L (Zheng et al., 2011). Therefore, it is essential to treat any ferric ion contaminated water to a level below the permissible limit of 0.3 mg/L (WHO, 2017). The overdose of iron in human body may cause anorexia, oliguria and diphasic shock, haemochromatosis, diabetes mellitus, liver cancer and cirrhosis (Li et al., 2016, Bhattacharyya and Gupta, 2006a). The adsorption of Fe (III) and Cr (VI) in wastewaters is a significant challenge. The adsorption technique is the easiest method used in the decontamination of heavy metals in discharged effluents. Some of its economic and technological advantages are, it is cheap and easy to operate, accessible and available, profitable and efficient, and effective than other techniques (Rao et al., 2014, Gupta et al., 2013).

According to Uddin (2017), different traditional and non-traditional adsorbents have been employed to remove heavy metals. They include adsorption of copper, lead, chromium and nickel (Dim et al., 2020, Ridha et al., 2017, Rai et al., 2016), and iron (Khalil et al., 2013, Zheng et al., 2011, Yeddou and Bensmaili, 2007, Bhattacharyya and Gupta, 2006b, Wan et al., 2005). Several studies have shown that natural and modified adsorbent has been used to remove heavy metal pollutants. Their use for adsorption is due to their large pore volume and surface-area (Rabie et al., 2019). Agricultural wastes and clay minerals are used to remove heavy metals and inorganic pollutants (Bakalár et al., 2020). Recently some researchers like, Bazrafshan et al. (2017) investigated the use of Cydonia oblonga seed to remove Cr (VI) ions from aqueous solution. Balarak et al. (2016b), reported the treatment of *Azolla filiculoides* with tetraoxosuphate (VI) acid (H_2SO_4) for the removal of cadmium from aqueous solution. The result showed that Azolla Filiculoides could be an efficient adsorbent to remove Cd (II) from contaminated water. Additionally, Balarak et al. (2016a) also showed that barley husk a low-cost agricultural waste could be used to remove Cd (II) from aqueous solutions. In a similar study, Azarpira and Mahdavi (2016), investigated the use of Canola biomass for the adsorption of Cd (II) from aqueous solution in a batch system. Also, removing noxious nickel (II) was reported using a novel γ-alumina nanoparticle and multiwalled carbon nanotubes (Agarwal et al., 2016).

Clay minerals are natural and effective adsorbents, and acid treatment will enhance their adsorption capacity (Dim et al., 2020, Sejie et al., 2016). As a useful adsorbent material, clay has played a crucial role in decontamination of heavy metals in aqueous media. Clay a natural resource, has a great tendency to serve as an alternative adsorbent for decontamination of aquatic bodies. Its advantages include high cation exchange capacity, renewability, low-cost, excellent affinity, non-toxic, and it can be regenerated (Sarma et al., 2016). This material is available in large quantity and also has a high surface area. Previous studies reported that acid modification of local clay samples enhanced its adsorption for heavy metals (Dim et al., 2020, Sarma et al., 2016). Therefore, it becomes necessary to improve the adsorption capacity and expand local clay application beyond fine art and local pottery work. Thus, this study will characterize clay treated with hydrochloric and acetic acid to improve its utilization and commercial value of the local clay. The sourcing of natural material from local sources is advantageous because it will support the local economy and help lower environmental impact.

The different types of acids used for clay treatment include inorganic and organic acids such as hydrochloric, sulphuric, nitric, acetic, citric, oxalic and lactic acid. The treatment of clay with hydrochloric or sulphuric generates new surface acid sites quickly. However, hydrochloric acid is more effective in activating the local clay than sulphuric acid (Mokaya and Jones, 1995, Mahmoud and Saleh, 1999) and acetic acid preserve clay structure. It is effective in the generation of surface acid sites (Mahmoud and Saleh, 1999). Their choice depends on the type and nature of clay, acid concentration and activation time (Valenzuela-Diaz and Souza-Santos, 2001). They have advantages, including lower acid costs/unit mass of clay treated, lower production costs and environmentally friendly. In this study, the clay was treated with hydrochloric and acetic acid, to date no report on the use of the local clay for the adsorption of chromium and iron in real practical industrial textile wastewater.

The objectives of study are to examine the adsorption characteristic of clay treated with acids for Fe (III) and Cr (VI) removal in batch system. To explore the effect of treatment on the structure of clay; and investigate the effect of contact time, dosage, pH and temperature, and the isotherms, kinetics, and thermodynamics on the practical application of HMC and AMC in the removal of heavy metals from real industrial wastewater.

2. Materials and methods

2.1. Materials

The clay was obtained from Umunze, Anambra State, Nigeria, is mainly used by the locals for pottery and artwork. Analytical grade reagents include phosphoric acid, sodium hydroxide, hydrochloric acid, acetic acid and potassium iodide were purchased from merck chemical company. Textile industry in the community supplied the effluent used. The standard solutions of Cr and Fe were used as purchased from Sigma-aldrich Germany (99.99%) (1000 mg/L Cr in 2% nitric acid, prepared with high purity $(NH_4)_2Cr_2O_7$, HNO_3 and water and, 1000 mg/L Fe in 2% nitric acid, prepared with high purity Fe metal, HNO_3 and water).

2.2. Preparation of clay adsorbent

The raw clay (RC) treated with hydrochloric acid is (HMC), and acetic acid is (AMC). The clay minerals after crushing with a wooden mortar and a pestle. It was washed thoroughly with distilled water to remove any particles attached to its surface. The ground clay minerals were dried in an oven at 110 °C for 4 h. After pretreatment, 50 g of dried clay with 100 ml of 4 M hydrochloric and 2.5 M acetic acid solution, were stirred continuously for 30 min and left for 24 h. The suspension of clay was filtered, washed thoroughly and then dried at 85 °C overnight. After that, it was sieved to particle sizes of approximately 125 um and kept safe in a desiccator.

2.3. Characterization of modified clay

The Micromeritics ASAP 2020 measured the surface area and pore volume of the adsorbents. SEM-EDX (JEOLJSM 7600F) determined the morphology and elemental composition. X-Ray Fluorescence (XRF) and X-ray diffraction (XRD) analysis was done with a Model-PW2400 and MD 10 Randicon diffractometer, respectively. The cation exchange capacity (CEC) of clay was measured by mixing 5 ml of copper bisethylenediamine complex solution with 0.5 g clay in a 100 ml flask. After that diluted with distilled water to 25 ml. The mixture was agitated for 30 min in a thermostatic water bath shaker and centrifuged. The residual concentration was determined by mixing 5 ml of the complex with 5 ml of 0.1 M HCl to destroy the complex, followed by addition of 0.5 g KI per ml and then titrating it with 0.02 M $Na_2S_2O_3$ in the presence of starch as indicator. The CEC was calculated from values obtained (Bergaya and Vayer, 1997).

2.4. Adsorption study

The adsorption was conducted with batch method. 0.1 g of adsorbent was mixed in 250 ml conical flasks containing 50 ml of real wastewater and adjusted with 1.0 M NaOH or 1.0 M H_3PO_4. The content was agitated using water-bath shaker equipped with the controller of shaking and temperature (Jisico, model J-NSIL-R) at 190 rpm at room temperature for 120 min. After which is filtered, and the total iron and chromium concentration was determined by Atomic Absorption Spectroscopy (AAS) (Buck Scientific, model 210VGP) (Dokmaji et al., 2020). It is worthy to note that this method measures total Cr or Fe in solution, regardless of the oxidation state of the metal.

The content of Cr (VI) and Fe (III) were analysed by UV–vis spectrophotometer (Model UV-1601 Shimadzu) (Ahmed and Roy, 2009, Khamis et al., 2020). These parameters, as studied at the following experimental conditions. Contact time used are 10, 20, 30, 40, 50, 60, 90, and 120 min, adsorbent dose used are 0.1, 0.2, 0.3, 0.4 and 0.5 g, pH values was tested from 2 to 12 and temperatures were 25, 30, 35, 40 and 45 °C. Eq. (1) was applied to calculate the amount of heavy metals adsorbed, q_e (mg g^{-1}):

$$q_e = \frac{(C_0 - C_e)V}{W} \quad (1)$$

where C_0 (mg L^{-1}) is the initial concentrations of metal ions, Ce (mg L^{-1}) is the equilibrium concentration, V (L) is the volume of the solution, and W (g) is the mass of dry adsorbent. The removal efficiency (R) of metal ions represented by Eq. (2):

$$\%R = \frac{(C_0 - C_e)}{C_0} \times 100 \quad (2)$$

where C_e (mg L^{-1}) is the concentration of metal ions equilibrium.

2.5. Desorption study

The batch desorption studies tested the recoverability and reusability of HMC and AMC adsorbent. 30 ml of 0.1 N

Table 1 Chemical characterisation of RC, HMC and AMC.

Composition	Weight (%) RC	Weight (%) HMC	Weight (%) AMC
SiO_2	67.82	70.27	68.21
Al_2O_3	12.88	12.32	12.55
Fe_2O_3	6.68	5.17	6.42
Cr_2O_3	0.02	0.01	0.02
TiO_2	1.48	1.42	1.42
CaO	0.36	0.24	0.26
MgO	1.50	1.17	1.32
Na_2O	0.15	0.16	0.00
MnO	0.14	0.02	0.10
V_2O_5	0.03	0.01	0.04
K_2O	0.51	0.49	0.51
P_2O_5	0.12	0.12	0.13
LOI	7.92	7.79	8.31

HCl solution was contacted with adsorbents saturated with metal ions after the adsorption process. The mixture was shaken at 180 rpm for 120 mins, after which each sample was analysed for desorbed metal concentration (Fernández-Pazos et al., 2013). The percentage of desorption (Ds) of metal ions was expressed as Eq. (3), M_1 = amount of metal ions desorbed (mg), M_2 = amount of metal ions adsorbed (mg).

$$D_s(\%) = \left(\frac{M_1}{M_2}\right) \times 100 \quad (3)$$

3. Results and discussion

3.1. XRF results

XRF results, as presented in Table 1. The finding reveals that the major constituents in the clay are silica (SiO_2), alumina (Al_2O_3) and iron oxide (Fe_2O_3) containing an approximate percentage of 49.75, 9.20, and 6.94% respectively. The composition of copper, nickel, zinc, chromium, titanium, calcium, and manganese oxides was low, which conform to clay's chemical analysis (Bakhtyar and Shareef, 2013). From Table 1, the contents of the raw clay Al_2O_3, Fe_2O_3, MgO, CaO were 12.88, 6.88, 1.50, and 0.36 wt%. As can be seen that Al_2O_3, Fe_2O_3, MgO, CaO contents decreased; on the other hand, the content of silica oxide (SiO_2) content changed after treatment. The percentage of SiO_2 is 67.82% for the raw clay. However, it increased to 70.27% and 68.21% with treatment by hydrochloric acid and acetic acid. The increase resulted from removing impurities, replacing the exchangeable cations (K^+, Na^+ and Ca^{2+}) with hydrogen ions and leaching of Al^{3+}, Fe^{3+} and Mg^{2+} octahedral tetrahedral sites which exposes the edges of the clay particles (Tsai et al., 2007). It can also suggest that acid modification must have depleted the octahedral and interlayer and cations, affecting adsorbent efficiency (Nweke et al., 2015). The increase is mainly due to the elimination of exchangeable cations and generation of silica (Barrios et al., 1995). The significant increase in the surface area resulted from the treatment with mineral acids (Komadel and Madejova, 2006). The increase also caused the dissolution of the octahedral cations. The Fe^{3+} and Mg^{2+} were easy to dissolve by the acids, while Al^{3+} was difficult to dissolve. This behaviour is as a result of their positions in the structure of the clay. Mg^{2+} is found on the ribbons' edges, while Al^{3+} is at the octahedral ribbon centre (Güven, 1992). Besides, solubility plays a significant role in the changes; Al_2O_3 is less soluble in the acid medium than the MgO. The adsorbents' high mineral content and low carbonaceous matter confirmed the value of a loss on ignition obtained, 7.92 for RC, 7.79 for HMC and 8.31% for AMC (Yusuff et al., 2015).

3.2. BET analysis

The primary aim of acid activation of clay is to increase the adsorption area and void capacity because they affect adsorbent behaviour significantly. As exhibited by clay materials, the adsorption tendency corresponds to the available surface area (Elmoubarki et al., 2015). Furthermore, studies have shown that the relationship existing between a clay available area and its adsorption ability is directly proportional (Sarma et al., 2016, Elmoubarki et al., 2015).

As shown in Table 2, HMC and AMC have a surface area of 389.37 and 319.955 m^2/g, respectively. The effect of acid activation caused more surface creation, which resulted in about four-fold increment compared to RC (84.223 m^2/g). A similar effect in total pore volume (0.2168 and 0.2285 ml/g) for the modified clay in the ratio of 4:1 with raw clay. The surface area increased resulted from the removal of impurities, generation of silica, replacement of the exchangeable cations (K^+, Na^+ and Ca^{2+}) with hydrogen ions. The leaching of Al^{3+}, Fe^{3+} and Mg^{2+} from the octahedral and tetrahedral sites exposes the edges of clay particles (Edama et al., 2014, Tsai et al., 2007).

The CEC of the raw clay (RC) is 8.41 cmol/g, and acid treatment increased it to 22.29 cmol/g for HMC and 20.73 cmol/g for AMC, which is almost thrice the value of RC. The treatment of the clay resulted in the replacement of different cations with H^+ ions. The ion exchange capacity of clay minerals resulted in structural defects, broken bonds and structural hydroxyl transfers. Acid treatment increased the total number of exchange sites marginally (Bhattacharyya and Gupta, 2006a, Rodrigues, 2003).

3.3. SEM analysis

The SEM morphology of RC, HMC and AMC are shown in Fig. 1. The micrograph of RC (Fig. 1a) shows the presence of a mixture of large plates that appeared to have been formed by several flaky particles stacked together in the form of agglomerates. The HMC (Fig. 1b) and AMC (Fig. 1c) clay show a clear difference in structure with RC (Fig. 1a). Fig. 1b and c showed the effect of acid treatment on the clay samples. This acid opened the platelets and produced a more porous structure which caused an increase in surface area (Kumar et al. 2013). Their surfaces are irregular, rough, porous, and heterogeneous, a suitable property of an adsorbent (Mudzielwana et al., 2016). The significant changes in HMC and AMC after activation compared to RC, can be observed from their respective images. This observation is similar to reports in the literature on the treatment of clay (Sarma et al., 2016, Edama et al., 2014).

Table 2 Result of BET Analysis.

Samples	Surface area (m^2/g)	Pore volume (cc/g)	Pore size (nm)	CEC
RC	84.223	0.0527	2.115	8.41
HMC	389.370	0.2168	2.116	22.29
AMC	319.955	0.2285	2.126	20.73

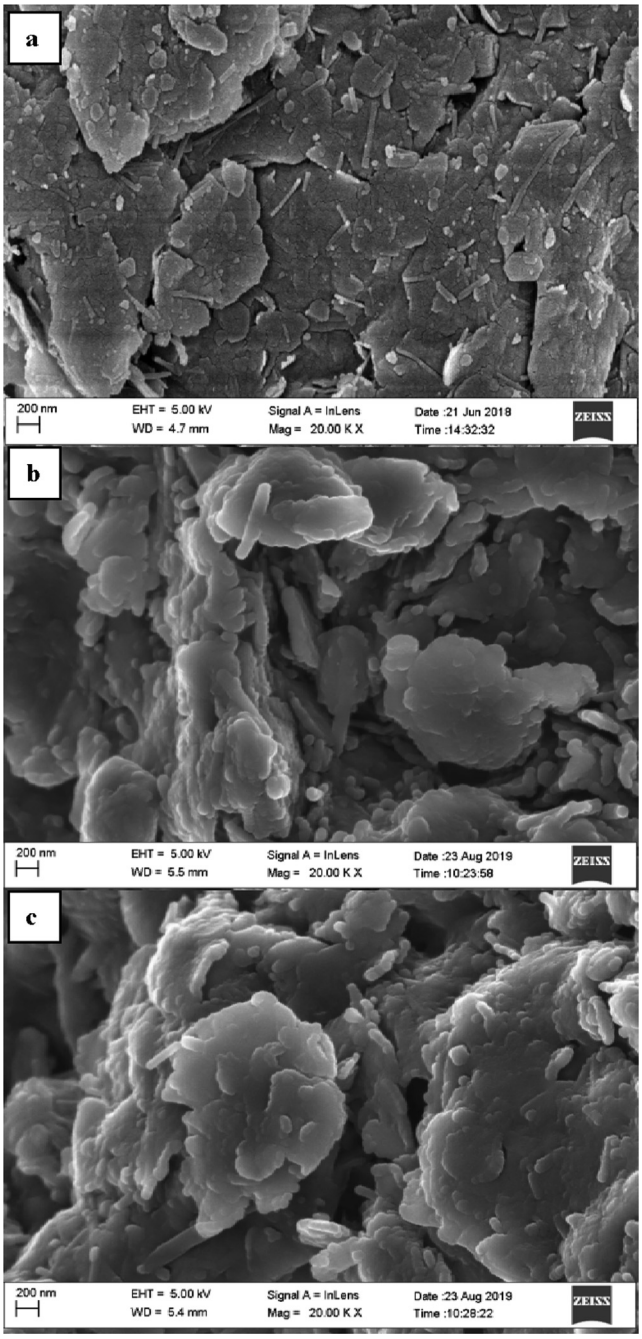

Fig. 1 SEM micrographs (a) RC (b) HMC and (c) AMC adsorbent.

3.4. XRD analysis

Fig. 2 show the diffractograms of the adsorbents. It displays spectra of the clay, (A) is montmorillonite, (B) is kaolinite and (C) is quartz, these species are related to clay fractions (Ayari et al., 2019, Sejie et al., 2016). The prominent peaks at 2θ = 25.2° and 28.65°, 30.2° and 53.45° are characteristic bands for quartz SiO_2 which is silica consisting of interconnected SiO_2 tetrahedra that build up a rigid three-dimensional network. The peaks at 2θ = 21.41°, 36.13°, 41.45°, 45.70°, 60.21° and 68.32° are characteristic of a kaolinite clay mineral (Sarma et al., 2016). The appearance of more kaolinite indicates the increase in the pore size of the treated clay. The transformation of the crystalline structure of clay leads to a decrease in peak intensity (Eren and Afsin, 2009).

3.5. Adsorption study

3.5.1. Effect of contact time

Sorption process depends on interaction time between adsorbent and adsorbates. The adsorption process, as performed in a time range of 10–120 min, and the results are shown in Fig. 3. The metal uptake increases rapidly with time up to saturation capacity at 50 min for HMC and gradually for 90 min for AMC. After that, the metal ion uptake became slow and significantly constant, suggesting the equilibrium time as 50 and 90 min for HMC and AMC. The maximum adsorption achieved at equilibrium time of 50 min for HMC is Cr (VI) (74.39%) and Fe (III) (89.93%), and 90 min for AMC are Cr (61.23%) and Fe (79.74%). In the adsorption process, equilibrium time is crucial for metal ion removal from solution. Its implementation can improve cost efficiency in adsorption technology. Rapid increase at the onset of adsorption process occurred because of the high solute concentration gradient and vacant pore voids. As the contact time increased metal uptake slows down because of the occupation of the available adsorption sites. The heavy metal movement into the pore surface will be slow due to few sites available; this will continue until equilibrium is achieved (Azouaou et al., 2010).

3.5.2. Solution pH

The pH was tested at 190 rpm, adsorbent dosage of 0.1 g and 25 °C., as shown in Fig. 4. The pH varied from 2 to 12. The percentage removal of the species increased as the pH increased for both adsorbents. The removal by adsorbent HMC and AMC shows a steady increase in both metal ions' pH value. The changing of the pH from 2 to 12 caused an increase in the removal of metals. HMC achieved the maximum removal of 79% Cr (VI) and 90% Fe (III) at pH 7.0 and AMC is 60% and 57% at pH 6.0, respectively. Maximum metal removal peaked at pH of 7.0 and 6.0 for HMC and AMC, suggesting the optimum pH values. At any pH, the HMC has a higher removal percent compared to the AMC.

However, beyond the maximum removal, the AMC equilibrium behaviour in removing metal species was constant. However, for HMC, Cr (VI) ion removal was constant, and Fe (III) showed a moment of stability, and a sudden rise in removal was observed (Boonamnuayvitaya et al., 2004). This behaviour could be the effect of competition from other contaminants, precipitation of complexes of chromium, Cr $(OH)_3$ and iron, Fe $(OH)_3$ at pH beyond 6 and 7. The insoluble complexes of precipitated metal hydroxides may appear as apparently higher metal ion removal (Srivastava et al., 2008, Hizal and Apak, 2006). According to Azouaou et al. (2010), the binding of metal ions is based on the theory of acid-base equilibria which is the dissociation of weak acid bonds within a pH range of 2–7. The formation of complexes of chromium and iron beyond pH 6.0 and 7.0 must have hindered the diffusion of Cr (VI) and Fe (III) ions to the clay surface resulting to concurrent adsorption and co-deposition (Bhattacharyya and Gupta, 2008). The increase in species adsorption in acidic medium was by electrostatic attraction between positively charged groups on the clay surface and

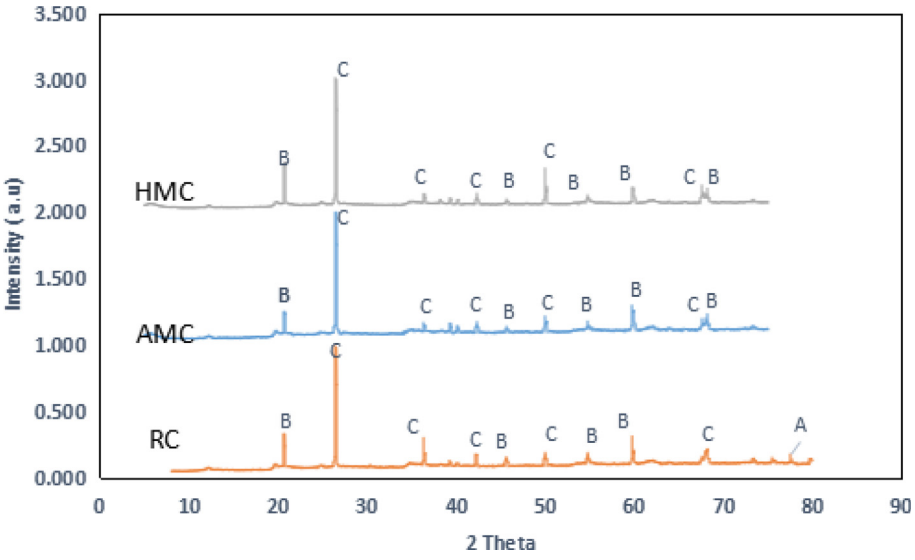

Fig. 2 XRD pattern of RC, AMC and HMC.

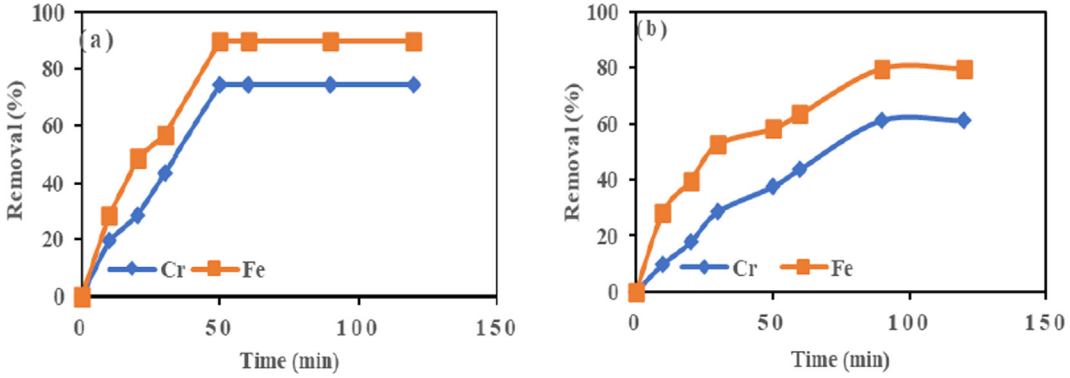

Fig. 3 Effect of contact time on adsorption of Cr (VI) and Fe (III) onto (a) HMC and (b) AMC at agitation speed = 190 rpm, Mass = 0.1 g, and temperature = 25 °C.

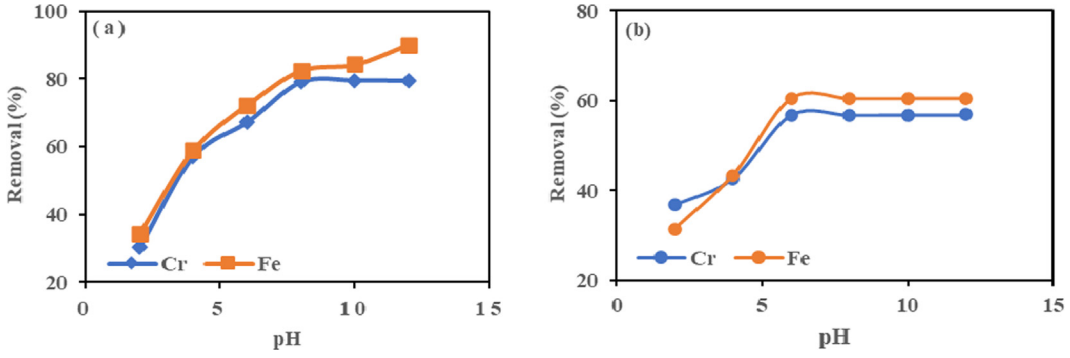

Fig. 4 Effect of pH on adsorption of Cr (VI) and Fe (III) onto (a) HMC and (b) AMC at agitation speed = 190 rpm, Mass = 0.1 g, and temperature = 25 °C.

oxyanions of Cr (VI), i.e., $HCrO_4^-$ anion and $Fe(OH)^{3+}$ (Padmavathy et al., 2016). At low pH, Fe (III) and Cr (VI) ions face stiff competition from H_3O^+ ions for the adsorption sites and consequently lead to low adsorption. The active sites on clay surface have weakly acidic properties (Boonamnuayvitaya et al., 2004; Padmavathy et al., 2016). These sites will gradually deprotonate at comparatively higher pH resulting in high metal ions uptake (Rai et al., 2016, Rangabhashiyam and Selvaraju, 2015, Taffarel and Rubio, 2009). The adsorption behaviour, as displayed by HMC and AMC, resulted from mechanisms such as

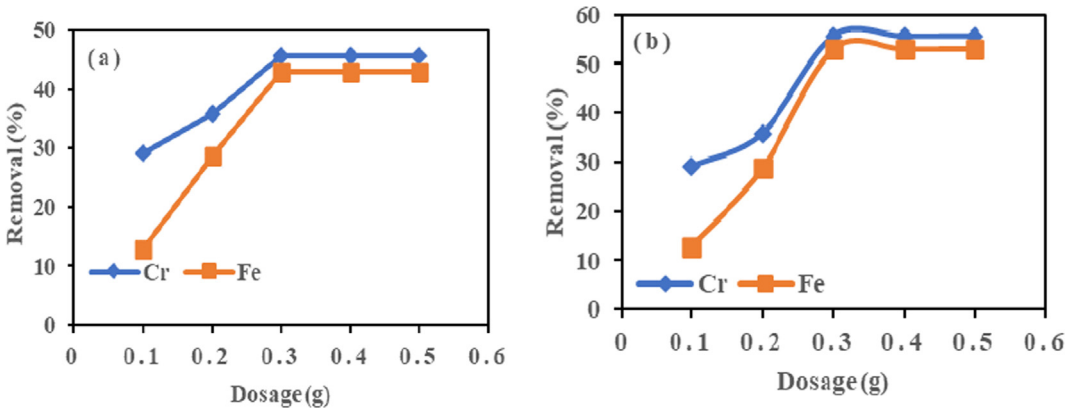

Fig. 5 Effect of adsorbent dosage on adsorption of Cr (VI) and Fe (III) onto (a) HMC and (b) AMC at agitation speed = 190 rpm, Mass = 0.1 g, and temperature = 25 °C.

ion exchange, chemical complexation, and electrostatic forces (Bhattacharyya and Gupta, 2008).

3.5.3. *Effect of adsorbent dose*

The effect of adsorbent dose test was chosen within 0.1–0.5 g, as seen in Fig. 5. The removal of metal ions increased with dosage for HMC and AMC adsorbent. The metal ion adsorbed by HMC increased with the amount of adsorbent until at 0.3 g, the maximum value was attained. However, the removal became steady beyond this point, suggesting an optimum dosage of 0.3 g for HMC, with maximum adsorption of 45.69% for Cr (VI) and 42.86% for Fe (III). On the other hand, for AMC, the removal percent also increased with the amount of adsorbent. The maximum removal of 55.69% for Cr (VI) and 52.91% for Fe (III) at 0.3 g is the optimum dosage after which removal percent decreased. From Fig. 5, percentage adsorption increased between 0.1 and 0.3 g; the dose increased the availability of adsorption sites. However, beyond 0.3 g, Cr (VI) and Fe (III) were few in the reaction medium to interact with the available surface area. Hence the adsorption gradually becomes constant or decreased, and additional adsorbent made no contribution (Simha et al., 2016).

3.5.4. *Effect of temperature*

As seen from Fig. 6, temperatures chosen for the test are 25, 30, 35, 40 and 45 °C. The sorbent HMC showed an increase in metal ions adsorption from 25 to 35 °C, (87.49–97.56%) for Fe (III) and (82.37–92.35%) for Cr (VI). The increased kinetic effect led to increased mobility of the adsorbates molecule as temperature increased. The high adsorption recorded indicates the process is endothermic. A further increase in temperature beyond 35 °C had no or insignificant effect, suggesting the optimum temperature of HMC as 35 °C.

Conversely, for AMC the removal of Fe (III) and Cr (VI) increased gradually. They reached percentage removal of (38.34–45.65%) for Fe (III) and (31.67–37.64%) for Cr (VI) from 25 to 35 °C, and sudden increase in percentage adsorption was recorded of (45.43–58.37%) for Fe (III) and (37.64–51.68%) for Cr (VI), from 35 to 40 °C. The penetration of vacant active sites caused an increase in temperature; this suggests an endothermic process (Yusuff et al., 2017). The maximum percent removed for Fe (III) and Cr (VI) are 58.97% and 51.72% with AMC at the optimum temperature of 40 °C. Fig. 6a and 6b show 35 °C and 40 °C as the optimum value for metal ion removal by HMC and AMC, respectively.

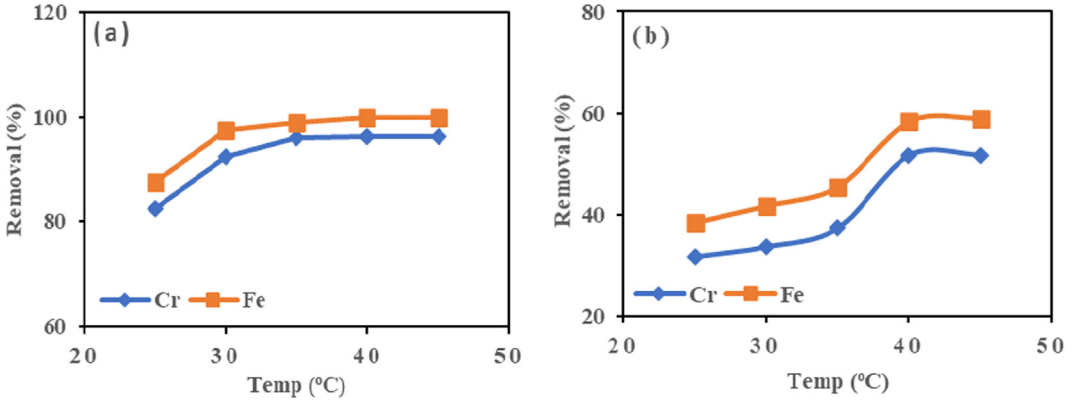

Fig. 6 Effect of temperature on adsorption of Cr (VI) and Fe (III) onto (a) HMC and (b) AMC at agitation speed = 190 rpm, Mass = 0.1 g.

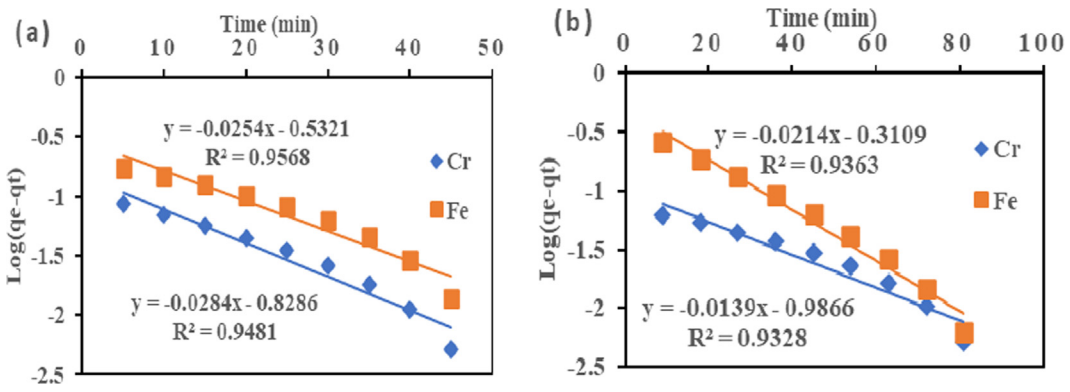

Fig. 7 Pseudo-first order for adsorption of Cr (VI) and Fe (III) onto (a) HMC and (b) AMC.

Table 3 Kinetic parameters for adsorption of Cr (VI) and Fe (III) onto HMC and AMC.

Pseudo-first-order kinetics												
Metal ions	HMC						AMC					
	$q_e$exp (mg/g)	$q_e$cal (mg/g)	k_1 (min^{-1})	R^2	SSE	χ^2	$q_e$exp (mg/g)	$q_e$cal (mg/g)	k_1 (min^{-1})	R^2	SSE	χ^2
Cr (VI)	0.1034	0.4367	0.0654	0.9481	0.1111	0.254	0.0713	0.2682	0.0320	0.9328	0.03876	0.1445
Fe (III)	0.2030	0.3504	0.0707	0.9568	0.0217	0.0619	0.0356	0.2641	0.0329	0.9363	0.05221	0.1976
Pseudo-second-order kinetics												
	$q_e$exp (mg/g)	$q_e$cal (mg/g)	k_2 (g. $mg^{-1}mn^{-1}$)	R^2	SSE	χ^2	$q_e$exp (mg/g)	$q_e$cal (mg/g)	k_2 (g. $mg^{-1}mn^{-1}$)	R^2	SSE	χ^2
Cr (VI)	0.0713	0.0729	1.679	0.999	2.56E-6	3.51E-5	0.0322	0.0582	0.0172	0.999	0.000676	0.0116
Fe (III)	0.2030	0.1334	0.526	0.998	0.00484	0.0362	0.3577	0.1394	0.0833	0.999	0.0476	0.1333

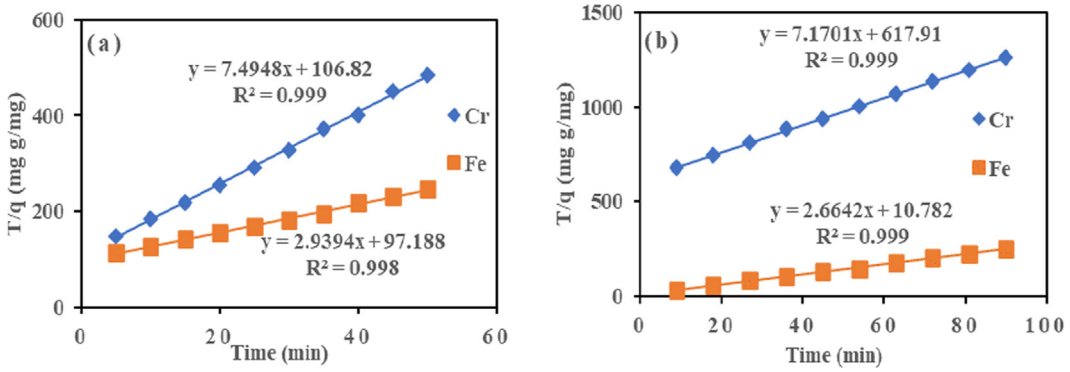

Fig. 8 Pseudo-second order for adsorption of Cr (VI) and Fe (III) onto (a) HMC and (b) AMC.

3.6. Kinetic study

The pseudo-first-order Eq. (4) and pseudo-second-order Eq. (5) was used to understand the adsorption dynamics with time for the ions system. As presented in Fig. 7 and Table 3, the R^2 value of 0.9481 and 0.9568 (Cr (VI) and Fe (III)), and 0.9328 and 0.9363 (Cr (VI) and Fe (III)) as obtained for the pseudo-first-order model. The correlation coefficients (R^2) values for the pseudo-first-order kinetic model were lower than second order. The value indicates that the first-order model did not accurately describe Cr (VI) and Fe (III) adsorption onto HMC and AMC. While R^2 values of pseudo-second-order for HMC and AMC adsorbents were 0.999 and 0.998 (Cr (VI) and Fe (III)), and 0.999 and 0.999 (Cr (VI) and Fe

(III)) respectively (Fig. 8 and Table 3). The calculated correlation coefficient (R^2) was high and very close to one for the pseudo-second-order kinetic model. The value illustrated good linearity with R^2 above 0.99. It demonstrated that the adsorption capacity was proportional to the number of active sites occupied on HMC and AMC. High regression coefficient (R^2) value conformed with the pseudo-second-order kinetic model (Bhattacharyya and Gupta, 2006a; Bhattacharyya and Gupta, 2006b; Al-Anber, 2015). Besides the higher regression coefficient (R^2) value, the lowest SSE and $\square^2$ values in the two error functions support the R^2 values (Table 3). This confirmed pseudo-second-order equation had the best fit; and are consistent with other reports in the literature (Akpomie and Dawodu, 2015).

$$\ln\left(\frac{q_e}{q_t}\right) = \ln q_e - k_1 t \tag{4}$$

$$\frac{t}{q_t} = \frac{1}{k_2 q_e^2} + \frac{t}{q_e} \tag{5}$$

where q_t is the amount of metal ions adsorbed (mg g^{-1}) at a given time t (min). q_e is the amount adsorbed at equilibrium (mg g^{-1}); k_1 (min^{-1}) and k_2 (g $mg^{-1}min^{-1}$) are the constants of first and second-order rate equation.

3.7. Adsorption isotherms study

The Langmuir model Eq. (6) and Freundlich model Eq. (7) in their linear form were employed to analyze the isotherm data to remove Cr (VI) and Fe (III) by HMC and AMC. The isotherms plots shown in Figs. 9–12 and the calculated parameters are in Table 4. High regression coefficient (R^2) values showed that Langmuir isotherm had a better fit than Freundlich. The adsorption occurred on a monolayer surface for all identical sorption sites (Rao and Uddin, 2014). The highest removal recorded for Cr (VI) and Fe (III) are 18.15 and 39.80 mg/g (HMC), and 10.42 and 19.34 mg/g (AMC), this suggests HMC has adsorptive advantage than AMC. The R_L values show that HMC has a greater affinity for the two metals than AMC. The adsorption is favourable because all the R_L obtained lies between zero and one ($0 < R_L < 1$) (Ayari et al., 2019, Goher et al., 2015).

$$\frac{C_e}{q_e} = \frac{1}{K_L q_m} + \frac{1}{q_m} C_e \tag{6}$$

where q_e (mg g^{-1}) is the amount of metal ion adsorbed, q_m, represents complete monolayer adsorption of metal ions (mg g^{-1}), and K_L (L mg^{-1}) is the Langmuir constant.

$$\ln q_e = \ln K_F + \frac{1}{n} \ln C_e \tag{7}$$

where K_F (mg.g^{-1}) (Lg^{-1}) and n are the Freundlich adsorption constants.

The value of separation factor (R_L) indicates the effectiveness of adsorbent, and this is defined as represented in Eq. (8),

$$R_L = \frac{1}{1 + K_L C_0} \tag{8}$$

R_L will classify isotherm to be either, favourable ($0 < R_L < 1$), unfavourable ($R_L > 1$), reversible ($R_L = 0$) or linear ($R_L = 1$).

3.8. Error analysis

The fitting for best isotherm and kinetic model calculated by analyzing the regression coefficient (R^2). Nevertheless, the models' linearization has resulted in inherent bias to confirm the good fit (R^2) of models. We employed error functions, chi-square test (χ^2) and sum square error (SSE) to confirm the best-fit isotherm and kinetic models using Eqs. (9) and (10) (Batool et al., 2018). The experimental value is expressed as qe, exp, the calculated value as qe, cal, and the number of data points (n).

$$\text{SSE} : \sum_{i=1}^{n} (q_{e,cal} - q_{e,exp})_i^2 \tag{9}$$

$$\chi^2 : \sum_{i=1}^{n} \frac{(q_{e,exp} - q_{e,cal})^2}{q_{e,cal}} \tag{10}$$

Beside higher R^2 (Table 4 and Figs. 9 and 10), the confirmation of isotherms and kinetic models using error analysis was investigated. The lowest SSE and χ^2 value supported the R^2 values (Table 4). The value further suggests that the Langmuir model is very suitable (Akpomie and Dawodu, 2015).

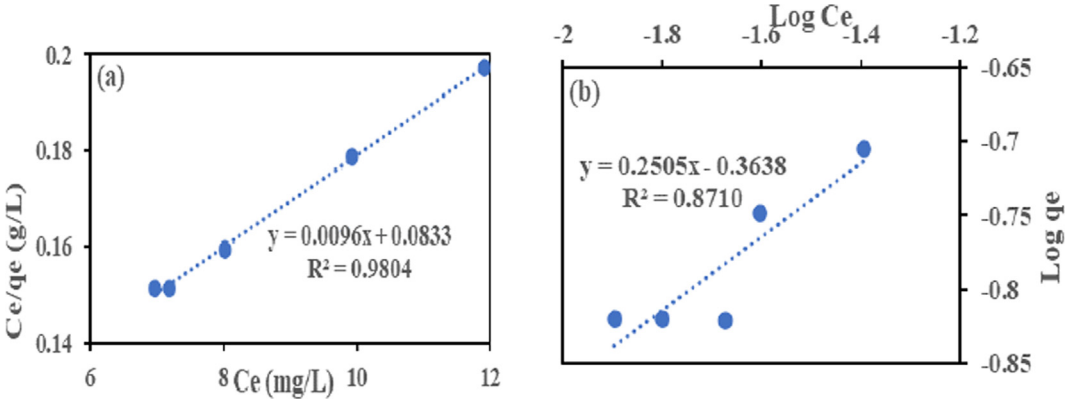

Fig. 9 (a) Langmuir and (b) Freundlich Isotherm for Cr (VI) adsorption onto HMC.

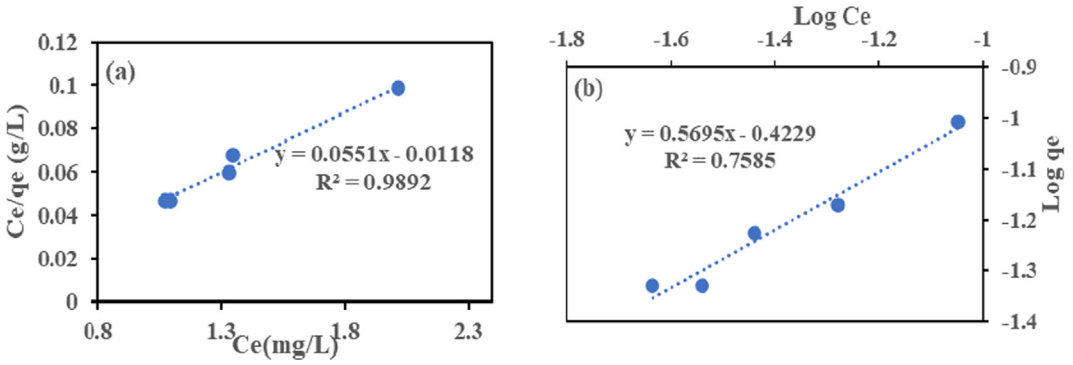

Fig. 10 (a) Langmuir and (b) Freundlich Isotherm for Fe (III) adsorption onto HMC.

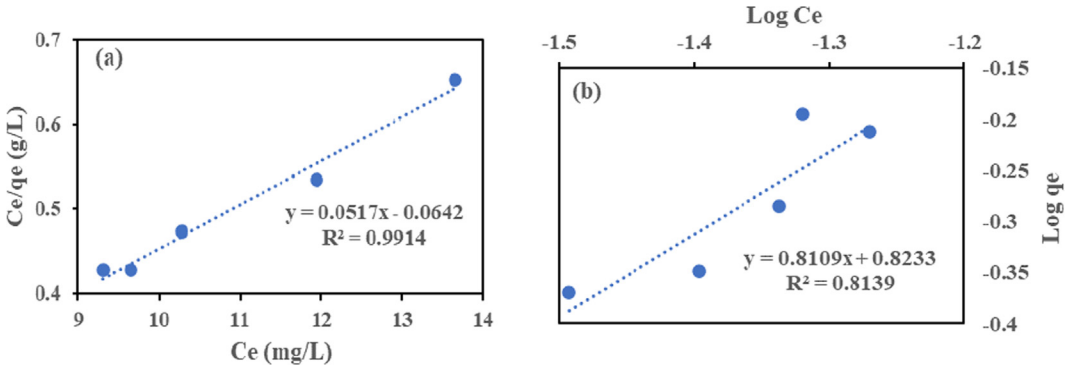

Fig. 11 Langmuir (a) and Freundlich (b) Isotherm for Cr (VI) adsorption onto AMC.

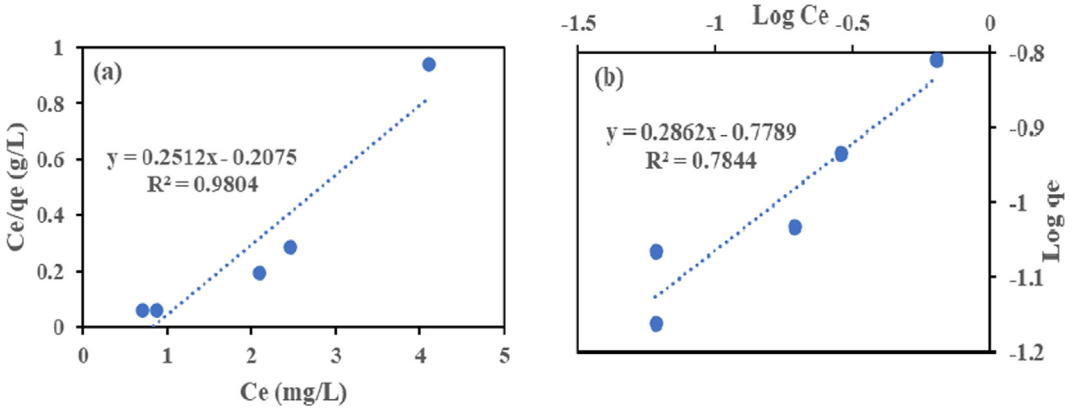

Fig. 12 Langmuir (a) and Freundlich (b) Isotherm for Fe (III) adsorption onto AMC.

A comparison of clay materials and their adsorption capacity for Fe (III) and Cr (VI) ions, are presented in Table 5. In Table 5, the Langmuir value for HMC and AMC compared with prior studies in the literature. It showed that both HMC and AMC displayed high adsorption capacity to signify improvement and suitability to remove heavy metals from wastewater.

3.9. Thermodynamic study

The thermodynamic parameters depend on the reaction process, and they can help in the detailed study of adsorption process mechanism. This experimental study considered different temperature values. The enthalpy (ΔH°) in kJ mol^{-1}, entropy (ΔS°) in kJ mol^{-1} K^{-1} and standard free energy (ΔG°) in kJ mol^{-1}, for sorption of metals onto adsorbents was determined with Eqs. (11)–(13). Eq. (13) was applied to analyze ln KC against 1/T plot, the slope obtained as enthalpy (ΔH°) and intercept as the entropy (ΔS°) respectively.

The reaction's thermal conditions examined at different temperatures of 25, 30, 35, 40 and 45 °C. The value of enthalpy change (ΔH°) is positive, which indicates an endothermic process. The enthalpy of HMC is 26.3 and 36.1 kJ mol^{-1}, and AMC is 66.7 and 27.9 kJ mol^{-1} respectively. This suggests that

Table 4 Isotherm parameters for adsorption of Cr (VI) and Fe (III) onto HMC and AMC.

Isotherm Parameter	HMC		AMC	
	Cr (VI)	Fe (III)	Cr (VI)	Fe (III)
Langmuir				
q_m(mg/g)	18.15	39.80	10.42	19.34
K_L (L/mg)	0.056	0.028	0.961	0.788
R_L	0.984	0.979	0.788	0.979
R^2	0.9804	0.9892	0.9914	0.9804
SSE	0.01137	0.00045	0.0179	0.0073
χ^2	0.03281	0.00132	0.1296	0.0190
Freundlich				
K_F (mg/g)(L/g)	1.526	7.264	1.439	2.278
n	1.76	0.356	3.991	1.233
R^2	0.8710	0.7585	0.8139	0.7844
SSE	0.0135	0.00345	0.0288	0.0097
χ^2	0.03782	0.0141	0.9936	0.0217

Table 5 Adsorption capacity of clay and other materials towards Cr (VI) and Fe (III).

Adsorbent	Metal ion	Langmuir q_m (mg/g)	References
HMC	Fe (III)	39.80	This study
AMC	Fe (III)	19.34	This study
Natural clay	Fe (III)	5.7	El-Maghrabi and Mikhail, 2014.
Brown algae	Fe (III)	60.67	Benaisa et al., 2016
Metal oxide nanocomposite	Fe (III)	22.03	Langeroodi et al., 2018
Acid activated clays	Fe (III)	30	Bhattacharyya and Gupta, 2006b.
Natural feldspar	Fe (III)	25	Al-Anber, 2015.
Zeolite	Fe (III)	10	Bakalár et al., 2020
Bentonite	Fe (III)	14	Bakalár et al., 2020
HMC	Cr (VI)	18.15	This study
AMC	Cr (VI)	10.42	This study
Purified carbon naontube	Cr (VI)	35.60	Hamzat et al., 2019
Leucocephala seed pod AC	Cr (VI)	26.94	Yusuff, 2019
Date press cake	Cr (VI)	28.28	Norouzi et al., 2018
Mango kernel	Cr (VI)	7.8	Rai et al., 2016
Natural material	Cr (VI)	15.67	Ksakas et al., 2015
Kaolin	Cr (VI)	11.60	Bhattacharyya and Gupta, 2006a.
Bentonite	Cr (VI)	48.83	Wanees et al., 2012.
Montmorillonite	Cr (VI)	28.9	Gupta and Bhattacharyya, 2012.

the interaction of metal ions with activated clay is endothermic (Bhattacharyya and Gupta, 2006a). The entropy change (ΔS^o) is positive, as measured at 298 K for Cr (VI) and Fe (III), HMC (0.058 and 0.159 kJ mol^{-1} K^{-1}) and AMC (0.239 and 0.154 kJ mol^{-1} K^{-1}). This signifies a strong affinity of ions for adsorbent and a high degree of randomness. The value of Gibbs free energy (ΔG^o) is negative, and it measures the spontaneity of a reaction process.

$$\Delta G^\circ = \Delta H^\circ - T\Delta S^\circ \tag{11}$$

$$\ln K_C = \frac{\Delta S^\circ}{R} - \frac{\Delta H^\circ}{RT} \tag{12}$$

$$\Delta G^\circ = -RT\ln K_c \tag{13}$$

where the universal gas constant (R) in $Jmol^{-1}$ K^{-1}, Temperature (T) in kelvin (K), and K_C is the adsorption equilibrium constant.

Table 6 shows that as temperature increased from 298 to 318 K, the free energy increased (become more negative) for both adsorbents. The increment indicates a favourable and energetically spontaneous reaction (Rao and Uddin, 2014). The analysis shows that the process was characterized by high randomness and spontaneous endothermic (Gupta and Bhattacharyya, 2012, Bhattacharyya and Gupta, 2012).

3.10. Desorption study

The reusability and stability of HMC and AMC are essential in terms of large-scale application. Table 7 shows that the amount of Cr (VI) and Fe (III) removed after first and second cycle decreased slightly, but decreased significantly after the second cycle for the adsorbents. The reduction in efficiency is probably due to the adsorption process's repeated desorption process, which decreased its adsorption capacity (Yussuf, 2019). The maximum desorption efficiency recorded on HMC is 92.45 and 85.67% for Cr (VI) and Fe (III) and for AMC is 76.58 and 65.32% for Cr (VI) and Fe (III). The results show HMC and AMC's recyclability potential in removing Fe (III) and Cr (VI) ions from real wastewater. The process is economical because it provides an avenue for safe disposal or reuse of adsorbent (Fernández-Pazos et al., 2013).

4. Conclusions

In this study, the effect of hydrochloric acid and acetic acid on the locally sourced clay has been investigated successfully. The BET analysis indicates an increase in surface area and pore volume after treatment. The surface area increased from 84.223 m^2/g for (RC) to 389.37 m^2/g (HMC) and 319.955 m^2/g (AMC), total pore volume increased to 0.2168 and 0.2285 cm^3/g, respectively. The CEC value was 22.30 cmol/g (HMC) and 20.73 cmol/g (AMC). These results show similarity with XRF and SEM studies which shows disintegra-

Table 6 Thermodynamic parameters for adsorption of Cr (VI) and Fe (III) onto HMC and AMC.

Adsorbent	Adsorbate	Temp (K)	ΔH^o (kJ mol^{-1})	ΔS^o (KJ mol^{-1} K^{-1})	ΔG^o (kJ mol^{-1})
HMC	Cr (VI)	298	26.30292	0.057807	−0.9236
		303			−1.21267
		308			−1.5017
		313			−1.7907
		318			−2.0798
	Fe (III)	298	36.0811	0.159155	−11.3471
		303			−12.1428
		308			−12.9386
		313			−13.7344
		318			−14.5302
AMC	Cr (VI)	298	66.664	0.239359	−4.6643
		303			−5.8611
		308			−7.05789
		313			−8.25468
		318			−9.45148
	Fe (III)	298	27.8884	0.15356	−0.15356
		303			−0.27436
		308			−0.57408
		313			−0.87379
		318			−1.17351

Table 7 Desorption efficiency of Fe (III) and Cr (VI) ions after four cycles.

		Desorption efficiency (%)			
Adsorbents	Adsorbates	Cycle 1	Cycle 2	Cycle 3	Cycle 4
HMC	Cr (VI)	92.45	85.46	64.24	48.54
	Fe (III)	86.32	80.87	59.76	42.43
AMC	Cr (VI)	76.58	65.46	44.23	40.45
	Fe (III)	65.32	58.67	41.97	39.89

tion and a porous structure of the treated clay. XRD study of the treated clay also shows changes in the intensity of the bands. Langmuir isotherm conformed best for both adsorbate on HMC and AMC adsorbent. The high regression coefficient (R^2) value shows the pseudo-second-order model as the better fit. Also, the lowest value of SSE and χ^2 supported the claim. The Langmuir adsorption capacity of Cr (VI) and Fe (III) for HMC was 18.15 and 39.80 mg/g, for AMC was 10.42 and 19.34 mg/g. The maximum desorption efficiency recorded on HMC is 92.45 and 85.67% for Cr (VI) and Fe (III) and for AMC is 76.58 and 65.32% for Cr (VI) and Fe (III). The process is important because it provides an avenue for safe disposal or reuse of adsorbent. Acid modified clay has the potential to treat heavy metal contaminated wastewater.

Declaration of Competing Interest

The authors declare that they have no known competing financial interests or personal relationships that could have appeared to influence the work reported in this paper.

Acknowledgements

The authors will like to appreciate the following for their contribution in sample analysis: Dr François Cummings (SEM/EDS, Physics Department), University of Western Cape (UWC), South Africa, Dr Remy Bucher (XRD, ithemba Labs), and Prof. S. J. Moir (XRF, Scientific Services CC), Cape Town, South Africa.

Funding

This research did not receive any specific grant from funding agencies in the public, commercial, or not-for-profit sectors.

References

Agarwal, A., Tyagi, I., Gupta, V.J., 2016. Rapid removal of noxious nickel (II) using novel γ-alumina nanoparticles and multiwalled carbon nanotubes: kinetic and isotherm studies. J. Mole. Liquids 224, 618–623.

Ahmed, J., Roy, U.K., 2009. A simple spectrophotometric method for the determination of iron (II) aqueous solutions. Turk. J. Chem. 33, 709–726.

Akpomie, K.G., Dawodu, F.A., 2015. Treatment of an automobile effluent from heavy metals contamination by an eco-friendly montmorillonite. J. Adv. Res. 6, 1003–1013.

Al-Anber, M.A., 2015. Adsorption of ferric ions onto natural feldspar: kinetic modelling and adsorption isotherm. Int. J. Environ. Sci. Technol. 2, 139–150.

Ayari, F., Manai, G., Khelifi, S., Trabelsi-Ayadi, M., 2019. Treatment of anionic dye aqueous solution using Ti, HDTMA and Al/Fe pillard bentonite. Essay to regenerate the adsorbent. J. Saudi Chem. Soc. 23, 294–306.

Azarpira, H., Mahdavi, Y., 2016. Removal of Cd (II) by adsorption on agricultural waste biomass. Der Pharma Chemica. 8 (12), 61–67.

Azouaou, N., Sadaoui, Z., Djaafri, A., Mokaddem, H., 2010. Adsorption of cadmium from aqueous solution onto untreated coffee grounds: equilibrium, kinetics and thermodynamics. J. Hazard. Mater. 184, 126–134.

Bakalár, T., Kanuchová, M., Girová, A., Pavolová, H., Hromada, R., Hajduová, Z., 2020. Characterization of Fe (III) adsorption onto zeolite and bentonite. Int. J. Environ. Res. Public Health 17, 5718–5727.

Bakhtyar, K.A., Shareef, H.F., 2013. Using natural clays and spent bleaching clay as a cheap adsorbent for the removal of phenol in aqueous media. Int. J. Basic Appl. Sci. 13, 45–49.

Balarak, D., Azarpira, H., Mostafapour, F.K., 2016a. Thermodynamics of removal of cadmium by adsorption on Barley husk biomass. Der Pharma Chemica. 8 (10), 243–247.

Balarak, D., Joghataei, A., Azarpira, H., Mostafapour, F.K., 2016b. Isotherms and thermodynamics of cd (II) ion removal by adsorption onto azolla filiculoides. Int. J. Pharm. Technol. 8 (3), 15780–15788.

Barrios, M.S., Gonzalez, L.V.F., Vicente, M.A., 1995. Acid activation of a polygorskite with HCl: Development of physic-chemical textural and surface properties. Appl. Clay Sci. 10, 247–258.

Batool, F., Akbar, J., Iqbal, S., Noreen, S., Bukhari, S.N.A., 2018. Study of isothermal, kinetic, and thermodynamic parameters for adsorption of cadmium: an overview of linear and nonlinear approach and error analysis Article ID 3463724, 11 pages Bioinorganic Chem. Appl. 2018. https://doi.org/10.1155/2018/3463724.

Bazrafshan, E., Sobhanikia, M., Mostafapour, F.K., Kamani, H., 2017. Chromium biosorption from aqueous environments by mucilaginous seeds of Cydonia oblonga: kinetic and thermodynamic studies. Global NEST J. 19 (2), 269–277.

Benaisa, S., El Mail, R., Jbari, N., 2016. Biosorption of Fe (III) from aqueous solution using brown algae *Sargassum Vulgare*. J. Mater. Environ. Sci. 7 (5), 1461–1468.

Bergaya, F., Vayer, M., 1997. CEC of clays: Measurement by adsorption of a copper ethylendiamine complex. Appl. Clay Sci. 12, 275.

Bhattacharyya, K.G., Gupta, S.S., 2012. Adsorption of a few heavy metals on natural and modified kaolinite & montmorillonite. A review. Adv. Colloid Interface Sci. 140, 114–131.

Bhattacharyya, K.G., Gupta, S.S., 2008. Adsorption of Fe (III), Co (II) and Ni (II) on ZrO kaolinite and ZrO-montmorillonite surfaces in aqueous medium. Colloids Surf. A 317, 71–79.

Bhattacharyya, K.G., Gupta, S.S., 2006a. Adsorption of chromium (VI) from water by clays. Ind. Eng. Chem. Res. 45, 7232–7240.

Bhattacharyya, K.G., Gupta, S.S., 2006b. Adsorption of Fe (III) from water by natural and acid activated clays: studies on equilibrium isotherm, kinetics and thermodynamics of interactions. Adsorption 12, 185–204.

Boonamnuayvitaya, V.C., Tanthapanichakoon, C.W., Jarudilokkul, S., 2004. Removal of heavy metals by adsorbents prepared from pyrolyzed coffee residues and clay. Sep. Purif. Technol. 35, 11–22.

Ciopec, M., Davidescu, C.M., Negrea, A., Grozav, I., Lupa, L., Negrea, P., 2012. Adsorption studies of Cr (III) ions from aqueous solutions by DEHPA impregnated onto Amberlite XAD7-factorial design analysis. Chem. Eng. J. 90, 1660–1670.

Dim, P.E., Olu, S.C., Okafor, J.O., 2020. Kinetic and thermodynamic study of Adsorption of Cu (II) and Cr (VI) ion from industrial effluent onto kaolinite clay. J. Chem. Technol. Metall. 55, 1057–1067.

Dokmaji, T., Ibrahim, T., Khamis, M., Abouleish, M., Alam, I., 2020. Chemically modified nanoparticles usage for removal of chromium from sewer water. Environ. Nanotechnol. Monit. Manage. 14, 103–110.

Edama, N.A., Sulaiman, A., Hamid, K.H.K., Rodhi, M.N.M., Musa, M., Rahim, S.N.A., 2014. The effect of hydrochloric acid on the surface area, morphology and physico-chemical properties of Sayong Kaolinite clay. Key Eng. Mater. 594, 49–56.

El-Maghrabi, H.H., Mikhail, S., 2014. Removal of heavy metals via adsorption using natural clay material. J. Environ. Earth Sci. 4, 38–46.

Elmoubarki, R., Mahjoubi, F.Z., Tounsadi, H., Moustadraf, J., Abdennouri, M., Zouhri, A., ElAlban, A., Barka, N., 2015. Adsorption of textile dyes on raw and decanted Moroccan clays: kinetics, equilibrium and thermodynamics. Water Resour. Industry. 9, 16–29.

Eren, E., Afsin, B., 2009. An investigation of Cu (II) adsorption by raw and acid activated bentonite. A combined potentiometric, thermodynamic, XRD, IR, DTA study. J. Hazardous Mater. 151, 682–691.

Fernández-Pazos, M.T., Garrido-Rodriguez, B., Nóvoa-Muñoz, J.C., Arias-Estévez, M., Fernández-Sanjurjo, M.J., Núñez-Delgado, A., Álvarez, E., 2013. Cr (VI) adsorption and desorption on soils and biosorbents. Water Air Soil Pollut. 224, 1366. https://doi.org/10.1007/s11270-012-1366-3.

Goher, M.E., Hassan, A.M., Abdel-Moniem, I.A., Fahmy, A.H., Abdo, M.H., El-sayed, S.M., 2015. Removal of aluminium, iron and manganese ions from industrial wastes using granular activated carbon and Amberlite IR-120H, Egypt. J. Aquat. Res. 41, 155–164.

Gupta, S.S., Bhattacharyya, K.G., 2012. Adsorption of heavy metals on kaolinite and montmorillonite: a review. PCCP 14, 6698–6723.

Gupta, V.K., Kumar, R., Nayak, A., Saleh, T.A., Barakat, M.A., 2013. Adsorptive removal of dyes from aqueous solution onto carbon nanotubes: a review. Adv. Colloid Interface Sci. 193, 24–34.

Güven, N., 1992. Molecular aspects of clay-water interactions, in the clay-water interface and its rheological implications. In N. Güven, Clay Mineral. Society. Workshop Lecture 4, 1–79.

Hamzat, W.A., Abdulkareem, A.S., Bankole, M.T., Tijani, J.O., Kovo, A.S., Abubakre, O.K., 2019. Adsorption studies on the treatment of battery wastewater by purified carbon nanotubes (P-CNTs) and polyethylene glycol carbon nanotubes (PEG-CNTs). J. Environ. Sci. Health, Part A. https://doi.org/10.1080/10934529.2019.1596701.

Hizal, J., Apak, R., 2006. Modelling of cadmium (II) adsorption on kaolinite-based clays in the absence and presence of humic acid. Appl. Clay Sci. 32, 232–244.

Khalil, M.M.H., Al-Wakeel, K.Z., Rehim, S.S.A.E., Monem, H.A.E., 2013. Efficient removal of ferric ions from aqueous medium by amine modified chitosan resins. J. Environ. Chem. Eng. 15, 66–573.

Khamis, M.I., Ibrahim, T.H., Jumean, F.H., Sara, Z.A., Aallah, B.A., 2020. Cyclic sequential removal of Alizarin Red S Dye and Cr (VI) Ions using wool as a low-cost adsorbent. Processes 8, 556–564. https://doi.org/10.3390/pr8050556.

Komadel, P., Madejova, J., 2006. Acid activation of clay minerals. In: Bergaya, F., Theng, B.K.G., Lagalay, G. (Eds.), Developments in clay science: Handbook of clay science, vol. 1. Netherlands: Elsevier, Oxford. pp. 263–287.

Ksakas, A., Loqman, A., El Bali, B., Taleb, M., Kherbeche, A., 2015. The adsorption of Cr (VI) from aqueous solution by natural materials. J. Mater. Environ. Sci. 6 (7), 2028–2037.

Kumar, S., Panda, A.K., Singh, R.K., 2013. Preparation and characterisation of acids and alkali treated kaolin clay. Bullet. Chem. React. Eng. Catal. 8 (1), 61–69.

Langeroodi, N.S., Farhadravesh, Z., Khalaji, A.D., 2018. Optimisation of adsorption parameters for Fe (III) ions removal from aqueous solutions by transition metal oxide nanocomposite. Green Chem. Lett. Rev. 11 (4), 404–413.

Li, Y., Hu, X., Ren, B., Wang, Z., 2016. Removal of high-concentration Fe (III) by oxidized multiwall carbon nanotubes in a fixed bed column. Am. Chem. Sci. J. 10, 1–9.

Mahmoud, S., Saleh, S., 1999. Effect of acid activation on the de-tert-butylation activity of some Jordian clays. Clays Clay Miner. 47, 481–486.

Mokaya, R., Jones, W., 1995. Pillared clays and pillared acid-activated clay: a comparative study of physical, acidic and catalytic properties. J. Catal. 153, 76–85.

Mudzielwana, R., Gitari, W.M., Msagati, T.A.M., 2016. Characterisation of smectite rich clay soils: implication for groundwater defluoridation. South Afr. J. Sci. 112, 1–8.

Norouzi, S., Heidari, M., Alipour, V., Rahmanian, O., Fazlzadeh, M., Mohammadi-Moghadam, F., Nourmoradi, H., Goudarzi, B., Dindarloo, K., 2018. Preparation, characterisation and Cr (VI) adsorption evaluation of NaOH activated carbon produced from Date Press Cake; an agro-industrial waste. Bioresour. Technol. 258, 48–56.

Nweke, O.M., Igwe, E.O., Nnabo, P.N., 2015. Comparative evaluation of clays from abakaliki formation with commercial bentonite clays for use as drilling mud. Afr. J. Environ. Sci. Technol. 9 (6), 508–518.

Padmavathy, K., Madhub, G., Haseena, P., 2016. A study on effects of ph, adsorbent dosage, time, initial concentration and adsorption isotherm study for the removal of hexavalent chromium (Cr (VI)) from wastewater by magnetite nanoparticles. J. Environ. Technol. 24, 585–594.

Rabie, A.M., Abd El-Salam, H.M., Betiha, M.A., El-Maghrabi, H.H., Aman, D., 2019. Mercury removal from aqueous solution via functionalized mesoporous silica nanoparticles with the amine compound, Egypt. J. Pet. 28, 289–296.

Rai, M.K., Shahi, G., Meena, V., Meena, R., Chakraborty, S., Singh, R.S., Rai, B.N., 2016. Removal of hexavalent chromium Cr (VI) using activated carbon prepared from mango kernel activated with H_3PO_4. Resour. -Eff. Technol. 2, 63–70.

Rangabhashiyam, S., Selvaraju, N., 2015. Adsorptive remediation of hexavalent chromium from synthetic wastewater by a natural and $ZnCl_2$ activated Sterculia guttata shell. J. Mole. Liquid 207, 39–49.

Rao, R.A.K., Uddin, M.K., 2014. Kinetics and isotherm studies of Cd (II) adsorption from aqueous solution utilising seeds of bottlebrush plant (Callistemon chisholmii). Appl. Water Sci. https://doi.org/10.1007/s13201-014-0153-2.

Rao, R.A.K., Ikram, S., Uddin, M.K., 2014. Removal of Cr (VI) from aqueous solution on seeds of Artimisia absinthium (novel plant material). Desalin. Water Treat. 54, 3358–3371.

Ridha, M.J., Ahmed, A.S., Raoof, N.N., 2017. Investigation of the thermodynamic, kinetic and equilibrium parameters of batch biosorption of Pb (II), Cu (II) and Ni (II) from aqueous phase using low-cost biosorbent. Al-Nahrain J. Eng. Sci. 201 (1), 298–310.

Rodrigues, M.G.F., 2003. Physical and catalytic characterisation of smectites from Boa-Vista, Paraiba, Brazil. Ceramica 49, 146–150.

Sarma, G.K., Gupta, S.S., Bhattacharyya, K.G., 2016. Adsorption of Crystal violet on raw and acid-treated montmorillonite, K10, in aqueous suspension. J. Environ. Manag. 171, 1–10.

Sejie, F.P., Misael, S.N., Tabbiruka, D., 2016. Removal of methyl Orange from water by Adsorption onto modified local clay (kaolinite). Phys. Chem. 6 (2), 39–48.

Shen, Y.S., Wang, S.L., Huang, S.T., Tzou, Y.M., Huang, J.H., 2012. Biosorption of Cr (VI) by coconut coir: spectroscopic investigation on the reaction mechanism of Cr (VI) with lignocellulosic material. J. Hazard. Mater. 179, 160–165.

Simha, P., Banwasi, P., Mathew, M., Ganesapillai, M., 2016. Adsorptive resource recovery from human urine: system design, parametric considerations and response surface optimisation. Procedia Eng. 148, 779–786.

Srivastava, V.C., Mall, I.D., Mishra, I.M., 2008. Removal of cadmium (II) and zinc (II) metal ions from binary aqueous solution by rice husk ash. Colloids Surf. A: Physicochem. Eng. Asp. 312, 172–184.

Taffarel, S.R., Rubio, J., 2009. The removal of Mn (II) ions by Adsorption onto natural & activated Chilean zeolites. J. Miner. Eng.. 22, 336–343.

Tsai, W.T., Hsu, H.S., Su, T.Y., Lin, K.Y., Lin, C.M., Dai, T.H., 2007. The adsorption of cationic dye from aqueous solution onto acid-activated. J. Hazard. Mater. 147, 1056–1062.

Uddin, M.K., 2017. A review on the Adsorption of heavy metals by clay minerals, with special focus on the past decade. Chem. Eng. J. 308, 438–462.

Valenzuela-Diaz, F.R., Souza-Santos, P., 2001. Studies on the acid activation of Brazilian smectite clays. Quim. Nova 24, 345–353.

Wan, W.S., Ghani, S.A., Kamari, A., 2005. Adsorption behaviour of Fe (II) and Fe (III) ions in aqueous solution on chitosan and crosslinked chitosan beads. Biore Technol. 96, 443–450.

Wanees, S.A., Ahmed, A.M.A., Adam, M.S., Mohamed, M.W., 2012. Adsorption studies on the removal of hexavalent chromium-contaminated wastewater using activated carbon and bentonite. Chem. J. 2, 95–105.

WHO, 2017. Guidelines for Drinking-Water Quality, fourth ed., WHO, Press, Geneva.

Yeddou, N., Bensmaili, A., 2007. Equilibrium and kinetic of iron adsorption by eggshells in a batch system: Effect of temperature. Desalination 206, 127–134.

Yusuff, A.S., 2019. Adsorption of hexavalent chromium from aqueous solution by *Leucaena leucocephala* seed pod activated carbon: equilibrium, kinetic and thermodynamic studies. Arab J. Basic Appl. Sci. 26 (1), 89–102.

Yusuff, A.S., Olalekan, D.A., Oluwatosin, S.A., Olutoye, A.M., 2015. Synthesis and characterisation of anthill-egg Shell-Ni-Co mixed oxides composite catalyst for biodiesel production from waste frying oil. J. Bioprod. Bio. Refin. 12, 37–45.

Yusuff, A.S., Olateju, I.I., Ekanem, S.E., 2017. Equilibrium, kinetic and thermodynamic studies of the Adsorption of heavy metals from aqueous solution by thermally treated quail eggshell. J. Environ. Sci. Technol. 10 (5), 246–257.

Zheng, Y.J., Peng, Y.L., Le, H.C., Li, C.H., 2011. Separation and recovery of Zn, Fe and Mn in acid mine drainage. J. Central South Univ. Sci. Technol. 42, 1858–1864.